

## Software tool for thermographic inspection using multimodal fusing of thermal and visible images

INGENIERÍA ELÉCTRICA Y ELECTRÓNICA

### Herramienta software para inspección termográfica usando fusión multimodal de imágenes térmicas y de espectro visible

Rafael E. Ospina\*, Sergio D. Cardona\*, Bladimir Bacca-Cortes\*§

\*School of Electrical & Electronics Engineering, PSI Research Group,  
Universidad del Valle. Cali, Colombia.

§[bladimir.bacca@correounivalle.edu.co](mailto:bladimir.bacca@correounivalle.edu.co), [rafael.ospina@correounivalle.edu.co](mailto:rafael.ospina@correounivalle.edu.co), [desarrollo@hwdeco.co](mailto:desarrollo@hwdeco.co)

(Recibido: Octubre 06 de 2015 – Aceptado: Mayo 10 de 2016)

#### Abstract

Monocular cameras are commonly used in communication devices, entertainment, and industrial environments since they allow people to recognize rapidly scenes and objects. On the other hand, thermal cameras are mostly known in industrial environments to visualize the objects' thermic radiance but they lose their visual details. This work presents the design and implementation of a thermography inspection tool – INVIfusion – to fuse infrared and visual spectrum images. This tool includes three modules: image acquisition and calibration module, multimodal image fusion module, and report generation module. The main contribution of this work compared with other software inspection tools is INVIfusion supports cameras from different manufacturers (infrared and visible spectrum), having different field of view and spatial resolutions. To validate the suggested system's functionality and accuracy, quantitative and qualitative tests were performed considering different camera configurations. In all cases the thermal camera was a FLIR E320. Quantitative tests were performed measuring the mean symmetric re-projection error obtaining a maximum error of  $2.08 \pm 1.8$  pixels.

**Keywords:** *Multimodal image fusion, software inspection tool, thermography.*

#### Resumen

Las cámaras monoculares son comúnmente usadas en dispositivos de comunicación, y ambientes de entretenimiento e industriales ya que ellas permiten a la gente rápidamente reconocer diferentes escenas y objetos. Por otra parte, las cámaras térmicas son ampliamente conocidas en ambientes industriales para visualizar la radiación térmica de los objetos pero estas cámaras pierden los detalles visuales. Este trabajo presenta el diseño e implementación de una herramienta de inspección Termográfica que permite fusionar imágenes térmicas y de espectro visible – INVIfusion. Esta herramienta incluye 3 módulos: el módulo de adquisición de imágenes y calibración, el módulo de fusión de imágenes, y el módulo de generación de reportes. La principal contribución de este trabajo en comparación con otros aplicativos de inspección es que INVIfusion soporta diferentes cámaras de diferentes fabricantes (espectro visible o térmico), teniendo diferentes campos de visión y resoluciones espaciales. Para validar la funcionalidad y precisión del sistema propuesto, pruebas cuantitativas y cualitativas fueron realizadas considerando diferentes configuraciones de cámaras. En todos los casos la cámara térmica fue una FLIR E320. Pruebas cuantitativas fueron realizadas midiendo el error de re-proyección simétrico normalizado obteniendo un máximo error de  $2.08 \pm 1.8$  pixeles.

**Palabras clave:** *Fusión de imágenes, herramienta software de inspección, termografía.*

## **1. Introduction**

The Earth will pass climate departure in 2047. In other words, the planet's coldest year on record before 2005 will turn into the hottest one (Yesner, 2013). Important contributors to this situation are the greenhouse gases. The International Energy Agency (IEA) estimates that urban areas contribute over 67% of global greenhouse gases and it is expected to rise to 74% by 2030 (Yesner, 2013). Then, cities have fundamental role in improving energy efficiency and reducing carbon emissions. To do so, there are many options such as efficient street lighting, green buildings, efficient public transportation, domestic removable energy, and reductions in traffic.

Energy efficiency in all sectors must be improved to reduce greenhouse gases. One of the most demanded methods to measure this energy efficiency is using building thermography inspections, civil structures (indoors or outdoors), electronic and electric equipment (Vidas & Moghadam, 2013). One tool used for such measurements are thermal cameras. They allow visualizing the infrared radiance of objects. Such cameras are also, the preferred method for non-invasive predictive and preventive maintenance. However, these cameras have low resolutions and limited field of views. On the other hand, standard cameras (monocular cameras) are very popular devices. They offer highly detailed and familiar images of the surroundings with wide field of views and high resolutions. Therefore, it could be a good option to conceive a thermography inspection software tool that combines the strengths of these two domains (thermal and visual spectrum).

This paper describes the design and implementation of INVIfusion. The former is a software tool for Thermographic inspections

which fuses thermal and visible images (Ospina-Cardona et al., 2015). INVIfusion supports any camera configuration composed by a monocular and thermal cameras, which after reviewing the state of art, it is an important contribution compared to other available Thermographic inspection software. INVIfusion uses the calibration module in order to extract the intrinsic and extrinsic parameters of the stereo setup. Using these parameters, the multimodal image fusion module can capture visual and thermal images to fuse them together either fully or partially. Finally, the report module consolidates the data gathered in the Thermographic inspection accordingly with C16.30 (ASTM International, 2011).

This work is developed in five sections as follows: Section 1.1 presents the state of the art; Section 1.2 shows the system configuration and assumptions made. The proposed method to fuse visual and thermal images is presented in Section 2. The software implementation details and requirements are presented in Section 3. Section 4 presents the results and tests performed. Finally, Section 5 shows the paper conclusions.

### **1.1 Related works**

Designing and implementing a Thermographic inspection tool that fuses infrared and visual images involves two main aspects to be discussed. One is the extrinsic calibration between any two cameras (infrared and visual spectrum), and the other is consolidating the calibration and inspection processes into a software tool. Considering these two aspects, Table 1 shows the state of the art of most relevant works related with this work. One part of the table will contain the state of the art regarding calibration methods for hybrid camera systems (thermal and visual spectrum) while the other will display the state of the art about Thermographic software tools.

**Table 1.** State of the art in calibration hybrid camera systems (thermal and visual spectrum), and thermography software tools.

<i>Calibration of Hybrid Camera Systems</i>						
<i>Reference</i>	<i>Camera Setup</i>	<i>Calibration Pattern</i>	<i>Intrinsic Calibration</i>	<i>Extrinsic Calibration</i>		
(Prakash et al., 2006)	2 IR cameras	Check board grid heated by reflector	(Bouguet, 2013)	3D reconstruction using Epipolar geometry		
(St-Laurent et al., 2010)	IR and RGB camera	Board with holes and rear heat source	(Bouguet, 2013)	Optical axis alignment and FOV ratio		
(Senya et al., 2011)	IR and RGB camera	Board with holes and rear heat source and check board	(Bouguet, 2013)	(Bouguet, 2013)		
(Yang & Chen, 2011)	2 RGB cameras, IR camera and structured light	Projected check board and IR LEDs.	(Bouguet, 2013)	DLT like algorithm and Levenberg-Marquardt optimization		
(Ursine et al., 2012)	IR and RGB camera	Check board using wood and copper	(Bouguet, 2013)	Pixel to pixel alignment		
(Vidas et al., 2013)	RGB-D and IR camera	Check board with thermal mask and different emissivity background	(Zhang and Way, 1999)	3D line correspondence		
(Strandemar, 2013)	IR and RGB camera	N/A		Normalize resolutions, edge extraction and fuse them.		
(Ma et al., 2016)	Datasets	Not needed	Not needed	Gradient transfer function		
(Kim et al., 2016)	Datasets	Not needed	Not needed	Patch clustering-based dictionary		
(Zhao et al., 2016)	Datasets	Not needed	Not needed	Multi-window visual saliency		
<i>Thermography Software Tools</i>						
<i>Prop./Software</i>	<i>SmartView (Fluke, 2015b)</i>	<i>FLIR Tools (Fluke, 2015a)</i>	<i>DuoVision (Trotec, 2015)</i>	<i>IR Analyzer (Infrared, 2015)</i>	<i>IrSoft (Testo, 2015)</i>	<i>TermUV (Benitez et al., 2005)</i>
Camera image acquisition	YES	YES	YES	YES	YES	NO
Reports templates	YES	YES	YES	YES	YES	NO
Video IR	YES	YES	NO	YES	YES	NO
Changing IR parameters	YES	YES	YES	YES	YES	NO
Temperature analysis	YES	YES	YES	YES	YES	NO
Image processing tools	NO	NO	NO	YES	NO	NO
IR / RGB fusion	YES	YES	YES	NO	YES	NO
Camera calibration	NO	NO	NO	NO	NO	NO
Advanced processing tools	NO	NO	NO	NO	NO	YES

The calibration of a hybrid camera system might be thought similar to stereo camera rig calibration problem. However, according to Ursine et al. (2012) it is not enough to know the relative translation and rotation between the two cameras, since other important problems must be considered such as field of view, sensor size, and resolution. As observed in Table 1, the intrinsic calibration process is performed in most cases using the method proposed in (Bouguet, 2013); nevertheless, all works show different approaches for the extrinsic calibration process. Another important aspect to classify these works is the calibration pattern used in Prakash et al. (2006), St-Laurent et al. (2010), Senya et al. (2011) and Yang & Chen (2011), in which active thermography was used to build the calibration pattern. In contrast, in Ursine et al. (2012) and Vidas et al. (2013), a calibration pattern which exploits the different emissivity values of different materials was used.

In Prakash et al. (2006) a stereo rig of two infrared cameras is used to reconstruct a 3D map of the surface temperature based on Epipolar geometry. In Vidas et al. (2013) the authors propose a hybrid systems composed by a RGB-D camera (Kinect) and infrared camera to perform a 3D thermal mapping. Although, this type of extrinsic calibration uses 2D or 3D line correspondences to estimate the relative transformation between cameras; its disadvantages are geometrical constraints that depend on the thermal contrast of 2D or 3D lines.

In St-Laurent et al. (2010), Senya et al. (2011) and Yang & Chen (2011), the calibration method depends on building a specific calibration pattern. In St-Laurent et al. (2010) optical axis alignment is performed with the assumption of parallel camera alignment; in addition, the extrinsic calibration only is valid at fixed target distances from the camera set. In Senya et al. (2011), everything depends on the calibration pattern, the authors do not detail any procedure to balance the camera field of view or resolution. The proposed method in Yang & Chen (2011), includes a complicated and expensive camera setup involving a stereo camera, an infrared camera and a LCD projector; this setup is used in conjunction with a calibration pattern over which

IR LEDs are placed and aligned to the horizontal lines projected from the LCD. The authors use this setup in order to recover 3D thermal and visual information, however, the working distance is short and not suitable for outdoors thermography. The work of Ursine et al. (2012), has two contributions, a brute force pixel to pixel alignment method in order to obtain the extrinsic parameters and the calibration pattern; and the calibration pattern design. This calibration pattern was implemented in this paper.

The calibration methods presented in Table 1 and described above have not been implemented into a thermography software tool. For this reason, the second part of Table 1 summarizes the state of the art of different Thermographic inspection software tools provided by infrared camera manufacturers. Software tools such as Trotec (2015) and Infrared (2015) offer manual overlapping methods to fuse thermal and visual images using the PC keyboard or mouse, however, this method does not always work since manual alignment methods do not consider the projective transformation involved. On the other hand Fluke (2015), Fluke (2015b) and Testo (2015), offer real automatic image fusing between thermal and visual images. However, the fusing technique is unknown and only works using the set of cameras provided by the manufacturer. All software tools presented in the second part of Table 1 are able to generate thermography reports, but most of them do not include image processing tools in order to improve the acquired images.

On the other hand, works such as Ma et al. (2016), Kim et al. (2016) and Zhao et al. (2016) follow a different approach. Despite the fact that these works are purely academic, and once the image registration process was performed, they automatically found properties in both images (infrared and visual spectrum) in order to fuse them, and generating a new composite image. In Ma et al. (2016) canny edges are extracted in both images and the registration is conceived as a minimization problem. In Kim et al. (2016) an image patch dictionary is built using principal component analysis to combine the multimodal images. And Zhao et al. (2016) propose the detection of saliency features in both images using sliding windows in order to fuse them.

Taking into consideration the previous software tools, it is worth noting that commercial and academic Thermographic inspection software tools require specific camera setups, and custom calibration methods. Therefore, this work presents a Thermographic inspection tool which is able to perform an automatic intrinsic and extrinsic camera calibration of any hybrid camera setup (thermal and visual spectrum); as well as, performing thermal and visual multimodal image fusion. In addition, other important requirements are: image processing tools to enhance thermal and visual images; a report module to consolidate thermography inspection results; and a friendly GUI (Graphical User Interface) to automate all these processes. The extrinsic camera calibration will be performed here by using a 2D homography based method, which is an unexplored method in the context of hybrid camera setups and its computation can be handled with good accuracy.

### 1.2 System configuration

Figure 1a shows the hardware system setup, where a FLIR E320 infrared camera and a monocular camera are placed in stereo configuration using

a tripod and a support bracket. The FLIR E320 camera outputs an analog video signal which is digitalized using an EasyCap DC60+ converter. In this work different monocular cameras were used by turns as follows: Kodak M532, Genius iSlim 1300V2, and Sharp YH7B50. Thermal and visual images were acquired using a Laptop computer. It is worth noting that the base line between cameras was as short as possible in order to achieve the highest FOV overlaps.

Figure 1b shows the calibration pattern built considering the work of Ursine et al. (2012). The calibration pattern was constructed using two different materials with different emissivity such as wood and copper. The wood background measuring 94.5cm by 76.5cm; small squares of copper measuring 8cm by 8cm and 0.3cm of thickness were placed on the wood base. Then, the wood background was painted in black as observed in Figure 1b. The benefits of this particular arrangement are to have a reasonable difference of emissivity without heating the calibration pattern. Also, it allows getting high contrast images using the infrared and visual spectrum camera.



a.



b.

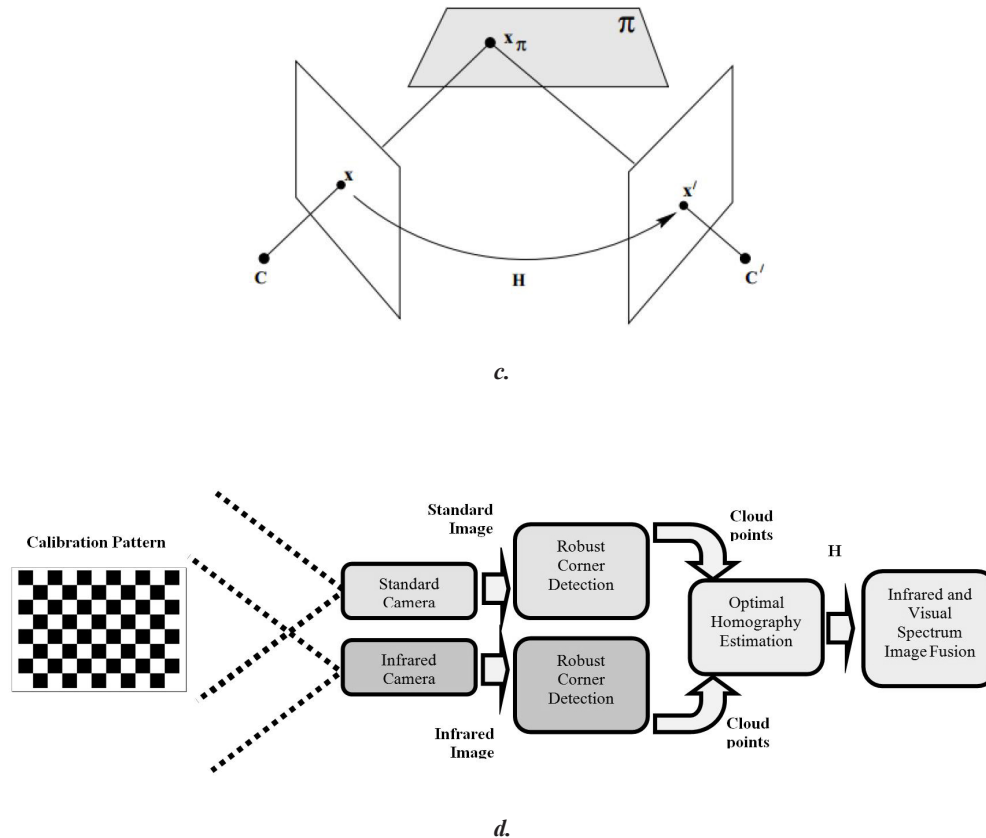


**Figure 1.** a) Image acquisition: FLIR E320 infrared camera, monocular camera, tripod with bracket for two cameras and laptop. b) Calibration pattern. c) Homography induced by a plane. d) Block diagram showing the pipeline process to compute the homography.

2. Thermal and visible images multimodal fusion  
 This section presents the INVIfusion 1.0 approach to fuse thermal and visible images. To do so, the process has been summarized in two main steps. First intrinsic camera calibration for both cameras, and second the homography robust estimation to project visual data between cameras. These two steps are illustrated in the next segments.

### 2.1 Calibration process

Obtaining the intrinsic calibration parameters of both the infrared camera and the visual spectrum camera are essential in order to project visual data between them. To do so, this process implemented the calibration methods suggested in Zhang (2000) and Bouguet (2013), which are currently available in OpenCV (OpenCV, 2014b). However, these methods were embedded into the GUI and

modified to achieve a better accuracy when the calibration pattern corners are detected. These corners are detected in two sequential steps, first a search window of 11x11 pixels was used; then, using those corners previously found a second window of 5x5 pixels was applied.

The GUI consolidates the intrinsic calibration process as previously stated. This process uses 10 different images pairs of the calibration pattern as described in Section 1.2. The intrinsic calibration results for the cameras used in this work are shown as follow:

*FLIR E320* – X focus:  $799.351 \pm 3.8485$ , Y focus:  $805.764 \pm 3.299$ , principal point  $[x, y]$ :  $[221.414 \pm 4.9482, 142.774 \pm 4.9487]$ , distortion  $[K_1, K_2, K_3, K_4, K_5]$ :  $[0.6457 \pm 0.055, -1.567 \pm 0.027, 0.005 \pm 0.0027, 0.0375 \pm 0.0055, 0.011 \pm 0.0027]$ .

*Kodak M532* – X focus:  $261.004 \pm 1.2396$ , Y focus:  $261.513 \pm 1.2402$ , principal point  $[x, y]$ :  $[158.059 \pm 1.4881, 117.562 \pm 1.4875]$ , distortion  $[K_1, K_2, K_3, K_4, K_5]$ :  $[-0.094 \pm 0.0062, 0.3103 \pm 0.00624, -0.0021 \pm 0.0006, 0.0002 \pm 0.00012, -0.636 \pm 0.00624]$ .

*Genius 1300V2* – X focus:  $756.819 \pm 2.6529$ , Y focus:  $753.624 \pm 2.6531$ , principal point  $[x, y]$ :  $[311.339 \pm 3.979, 229.926 \pm 3.7136]$ , distortion  $[K_1, K_2, K_3, K_4, K_5]$ :  $[-0.4485 \pm 0.0265, 0.0874 \pm 0.0265, -0.006 \pm 0.0006, 0.0013 \pm 0.00058, 0.7114 \pm 0.0265]$ .

*Sharp YH7b50* – X focus:  $756.819 \pm 2.6587$ , Y focus:  $753.624 \pm 2.06609$ , principal point  $[x, y]$ :  $[311.339 \pm 3.797, 229.926 \pm 3.805]$ , distortion  $[K_1, K_2, K_3, K_4, K_5]$ :  $[-0.4485 \pm 0.0266, 0.0874 \pm 0.0271, -0.006 \pm 0.000272, 0.0013 \pm 0.00027, 0.7114 \pm 0.0268]$ .

## 2.2 Homography robust estimation and multimodal image fusion

Considering the state of the art presented in Section 1.2, it is worth noting that performing standard stereo calibration between both cameras (infrared and visual spectrum) is not enough for hybrid camera setups (Ursine et al., 2012). Since, it is not possible to perform an image rectification process without distorting the temperature information; besides, thermal sensors are not committed to the form of objects in the scene, then disparity maps can not be obtained with precision. For this reason, in this work the multimodal fusion of infrared and visual spectrum images is performed using the homography induced by a plane (Zisserman & Hartley, 2004). This concept is observed in Figure 1c, where a set of corresponding points laying in plane  $x\pi$  are projected in  $x$  and  $x'$ . Then, the map from  $x$  to  $x'$  is the homography  $H$  induced by the plane  $\pi$ . This mapping is expressed in Ec. (1).

$$x' = Hx \tag{1}$$

In order to compute  $H$  the standard 4 points algorithm is used (OpenCV, 2014a); however, this algorithm works if and only if  $H$  is compatible with the fundamental matrix  $F$ , since the set of correspondences must obey the Epipolar constraint (Zisserman & Hartley, 2004) as described in Ec. (2).

$$x'^T Fx = 0 \tag{2}$$

Combining Ec. (1) and Ec. (2) give Ec. (3) which is true for all  $x$ , then, a homography  $H$  must satisfies the constraint expressed in Ec. (4).

$$x^T H^T Fx = 0 \tag{3}$$

$$H^T F + F^T H = 0 \tag{4}$$

In practical terms, Ec. (4) is not satisfied when there are degenerate configurations of the 3D corresponding points as collinearities. Those degenerated configurations have to be avoided when selecting the corresponding points.

Figure 1d shows the process pipeline to estimate the homography induced by a plane using the calibration pattern. This process can be detailed as follows:

*Image Acquisition:* two views of the calibration pattern are captured using both cameras (infrared and visual spectrum).

*Point clouds:* using the Harris sub-pixel corner detection (Harris & Stephens, 1988; OpenCV, 2014a) the corresponding points are extracted. They are checked in order to avoid degenerate configurations.

*Normalization:* the corresponding points are normalized such that the centroid of the set of points is  $[0, 0]$  and the average distance is  $\sqrt{2}$ . This is performed computing a similarity transformation  $T$  (Zisserman & Hartley, 2004).

*Initial Guess:* using RANSAC, the initial guess of  $H$  is found. The former is obtained considering the large number of inliers using the Direct Linear Transformation (DLT) algorithm (Zisserman & Hartley, 2004). In addition, Ec. (3) and (4) are evaluated to check homography compatibility with the fundamental matrix.

*Optimal Estimation:* the Levenberg-Marquardt algorithm is used to minimize the re-projection error described in Ec. (5).

$$E_{rep} = \sum_i \left( x'_i - \frac{h_{11}x_i + h_{12}y_i + h_{13}}{h_{31}x_i + h_{32}y_i + h_{33}} \right)^2 + \left( y'_i - \frac{h_{21}x_i + h_{22}y_i + h_{23}}{h_{31}x_i + h_{32}y_i + h_{33}} \right)^2 \quad (5)$$

Where,  $h_{xx}$  corresponds to the homography matrix elements, and  $x'_i, y'_i, x_i$  and  $y_i$  are the corresponding points image coordinates.

*De-normalization:* this is done applying  $H_{Def} = T^T H T$ .

*Image data projection:* Once the homography was computed, all common points between both FOV of the infrared and visual spectrum cameras can be projected between views. This is possible since they satisfy the geometry constraint depicted in Figure 1c. It is worth noting that the visual spectrum resolution is normally bigger than the thermal image resolution, this causes that a reduced part of the visual spectrum image can be observed by the infrared camera.

Until now, the corresponding points to obtain  $H_{Def}$  belong to the calibration pattern and they are extracted automatically. This method using the calibration pattern is useful if the object of interest does not change its relative depth to the camera setup, this would not happened in standard calibration methods. Nonetheless, this assumption is hard to satisfy in real environments. Taking the previous factors in consideration, experimental work was performed in order to check if feature extracting methods such as SIFT (Lowe, 2004), SURF (Bay et al., 2008), and FREAK (Alahi et al., 2012) are useful to the purposes of this work and to perform an automatic homography calculation. Once experimental work was performed, the findings indicate that feature extracting and matching using these descriptors did not produce suitable results, since there were considerable differences in image resolution, image appearance, and the nature of image data in the hybrid camera setup. Therefore, in the INVIfusio 1.0 GUI, in case the object of interest is placed at different depth distance compared with the moment at which

the extrinsic calibration was performed using the calibration pattern, the user can select the corresponding points manually. It is important to remember that the minimum number of points to select is 4 and they have to satisfy the constraints defined in Ec. (4). In other words, non collinear points should be selected. In the INVIfusion 1.0, these requirements are tested automatically.

Once the homography was computed, the multimodal fusing approach implemented in this work was weighted average (Sroubek et al., 2007). This method is described in Ec. (6), and it allows combining the pixel information of both images to show a better description of the scene.

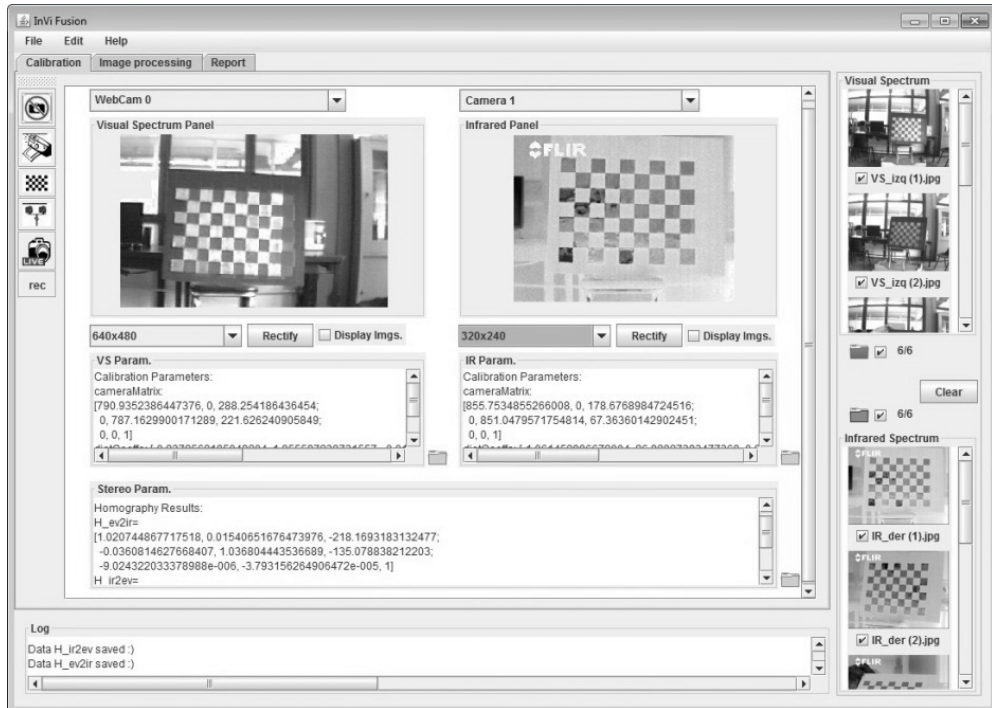
$$FI(x,y) = \alpha VS(x,y) + (1-\alpha)IR(x,y) \quad (6)$$

Where,  $x$  and  $y$  are the pixel coordinates,  $FI(x,y)$  is the resulting fused image,  $VS(x,y)$  is the visual spectrum image,  $IR(x,y)$  is the thermal image, and  $\alpha$  is the weight value for each image. The  $\alpha$  value is handled by the user using the INVIfusion 1.0 GUI.

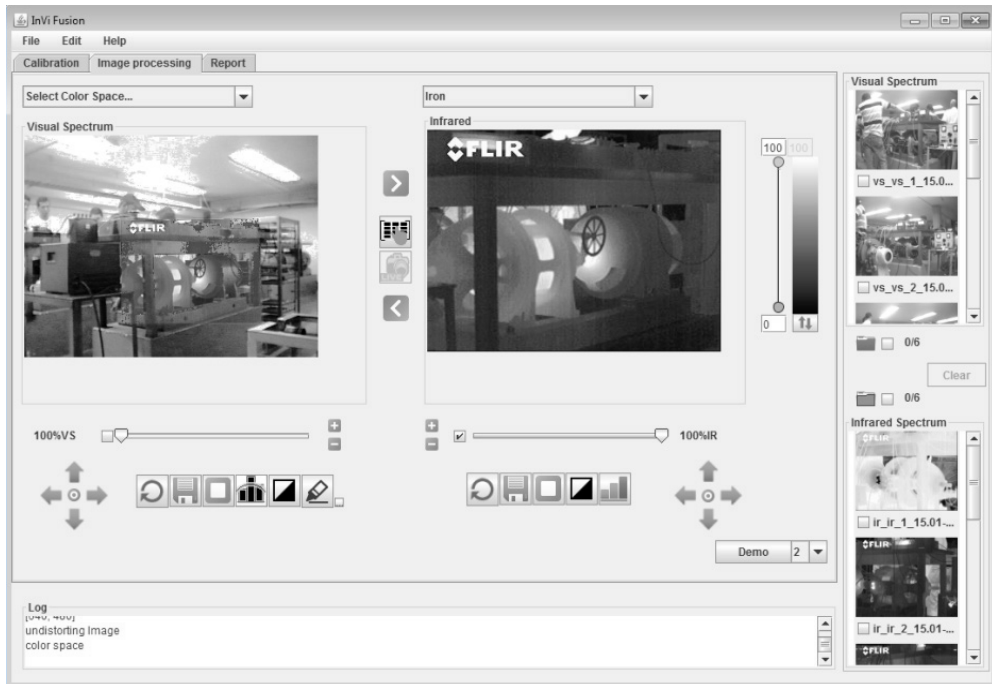
### 3. Software tool for thermographic inspection

This work proposes an automatic inspection software tool for hybrid camera systems called INVIFusion. This software tool was designed and implemented using RUP (Rational Unified Process) (Kruchten, 2003). Basically, INVIFusion contains three main modules: calibration, multimodal image fusion, and report generation. Figure 2a shows the GUI for the calibration module; that permits the users to carry out the following tasks: observing images from both cameras, taking image pairs for calibration, saving/loading/deleting images from the local workspace placed at right side, performing the cameras intrinsic calibration, and performing 2D homography computation.

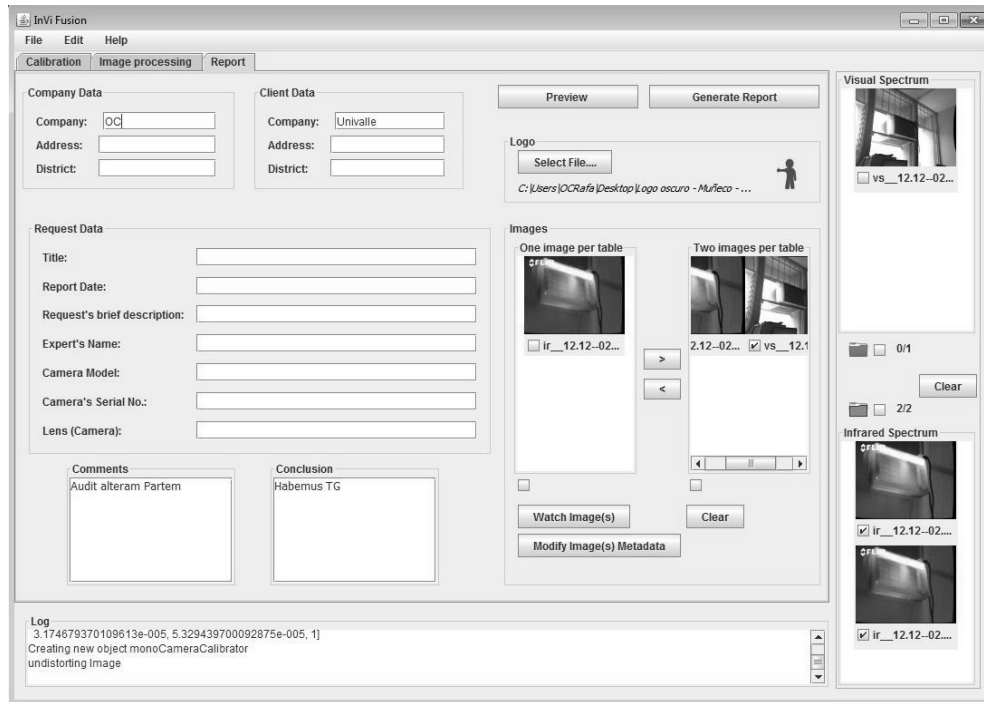




a.



b.



c.

**Figure 2.** a) *INVIFusion* calibration module. b) *INVIFusion* multimodal image fusion module. c) *INVIFusion* report module.

Figure 2b shows the multimodal image fusion module; on it users can perform tasks as projecting infrared images on visual spectrum images, these images can be projected using transparencies between 0 to 100%. This projection process can be performed in both ways, infrared to visual spectrum and visual spectrum to infrared. Also, selected areas of interest of visual spectrum or infrared images can be projected to the infrared or visual spectrum images. Other useful image processing functionalities available are: users can change the pseudo-color palette used to watch the infrared images, users can perform edge extraction on visual images and project them to the infrared image, and users can perform on-line thermal and visual spectrum video multimodal fusion.

Figure 2c shows the report generation module, which was designed and implemented to report the thermography for electrical equipment according to the ASTM International (2014). Additionally, the report generation module can print the visual

spectrum, infrared or fused images dragged from the workspace placed at right side of Figure 2c. An example of this format is shown in Section 4.2, according with E07.10 (ASTM International, 2014) this report must include: the images captured at fixed distance from target, the electrical equipment history must be available, the camera setup must be placed at safe location, different data from the camera setup must be included, personal data of whom did the inspection, electrical equipment datasheet, and date.

#### 4. Results and discussion

To validate the multimodal fusion method and the thermography software tool proposed in this work, three types of quantitative results were considered in this work. First, test results were performed to obtain the mean symmetric re-projection error (MSRE) once the homography matrix had been computed. Second, this work states that different hybrid camera setups are supported; then, intrinsic

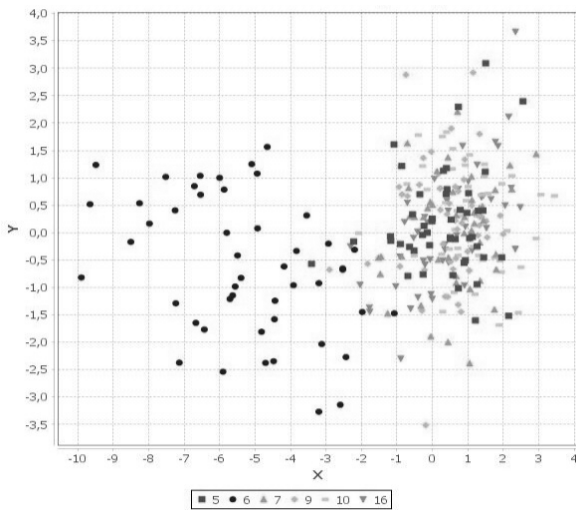
calibration, 2D homography computation, and MSRE tests were performed involving three different camera setups. Finally, qualitative results of thermal inspections were reported.

#### 4.1 Homography computation accuracy and comparison with other methods

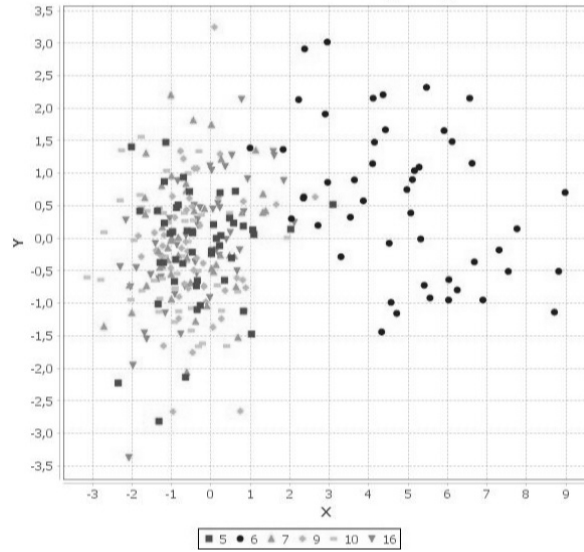
To quantify the multimodal image fusion method proposed in this work, the bidirectional projection of image data using the homography matrix must be evaluated. This evaluation is performed by considering the MSRE (Zisserman & Hartley, 2004). Then, being  $\mathbf{x}$  and  $\mathbf{x}'$  two corresponding points in image 1 and 2 respectively, the symmetric re-projection error is the difference between  $\mathbf{x}'$  and the projected point  $\mathbf{H}\mathbf{x}$ . This procedure is also made from image 2 to image 1, measuring the difference between  $\mathbf{x}$  and  $\mathbf{H}^T\mathbf{x}'$  as shown in Ec. (7)

$$E_{sim} = \frac{1}{N} \sum_{i=1}^N d(x'_i, Hx_i) + d(x_i, H^T x'_i) \quad (7)$$

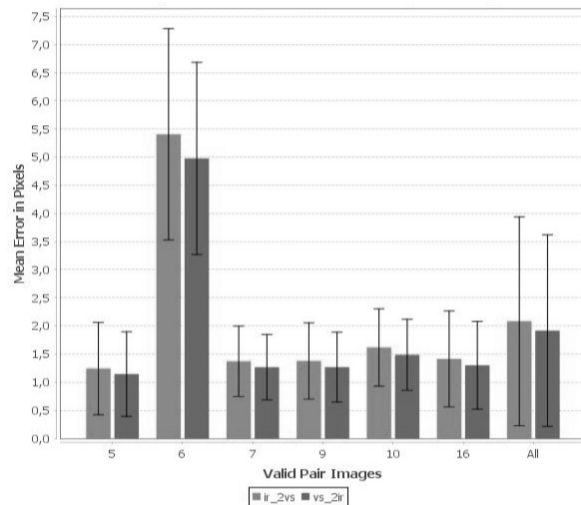
Where,  $N$  is the number of corresponding points and  $d()$  defines the Euclidean distance between two points. In this test, all the calibration image pairs were considered since they have the enough information to measure the MSRE, i.e. the corresponding points in each image belonging to the calibration pattern corners.



a.



b.



c.

**Figure 3.** a) Transfer error in pixels from infrared to visual spectrum image. b) Transfer error en pixels from visual spectrum to infrared image. c) Mean symmetric re-projection error (MSRE).

Figure 3a and 3b show the projection error from infrared to visual spectrum image and vice versa. The image pairs used to compute these results came from the image calibration pairs. Depending on the illumination conditions, some pairs are labeled as valid since the calibration pattern corners could be identified correctly in both images; in this case image pairs number 5, 6, 7, 8, 9, 10 and 16 were

used for the calibration purposes. Each set of points represent the error distribution corresponding to one calibration pair of images. The error is depicted in pixels around the target point. Figure 3c shows a bar diagram with uncertainty of the MSRE computed using Ec. (7) for each calibration pair. The first bar at each calibration pair shows the infrared to visual spectrum projection error, and the second bar at each calibration pair displays the visual spectrum to infrared projection error. The last bar depicts this error and uncertainty for all measurements. In Figure 3 can be observed that the proposed system shows a MSRE of  $2.08 \pm 1.8$  pixels in the worst case. It is worth noting that each time the hybrid camera setup is calibrated, the homography matrix is re-calculated and the MSRE graphs are displayed in the same form as depicted in Figure 3.

The software tool implemented in this paper is able to work with different hybrid camera setups; it means different infrared and visual spectrum cameras. Consequently, the intrinsic calibration process, the homography computation and the MSRE were performed for the following hybrid camera configurations: first, Sharp YH7B50 and FLIR E320 setup, obtaining a MSRE of  $1.995 \pm 1.16$  pixels; second, Kodak M532 and FLIR E320 setup, obtaining a MSRE of  $5.77 \pm 3.04$  pixels; and finally, Genius iSlim 1300V2 and FLIR E320 setup, obtaining a MSRE of  $2.083 \pm 1.803$  pixels. It is noteworthy that the MSRE in the first and last cases behaves well. Nevertheless, the MSRE ( $5.77 \pm 3.04$  pixels) in the Kodak M532 and FLIR E320 setup is greater due to high difference in the camera resolution. This means that the Kodak M532 has a sensor size of  $2048 \times 1536$  pixels while the FLIR E320 has  $320 \times 240$  elements.

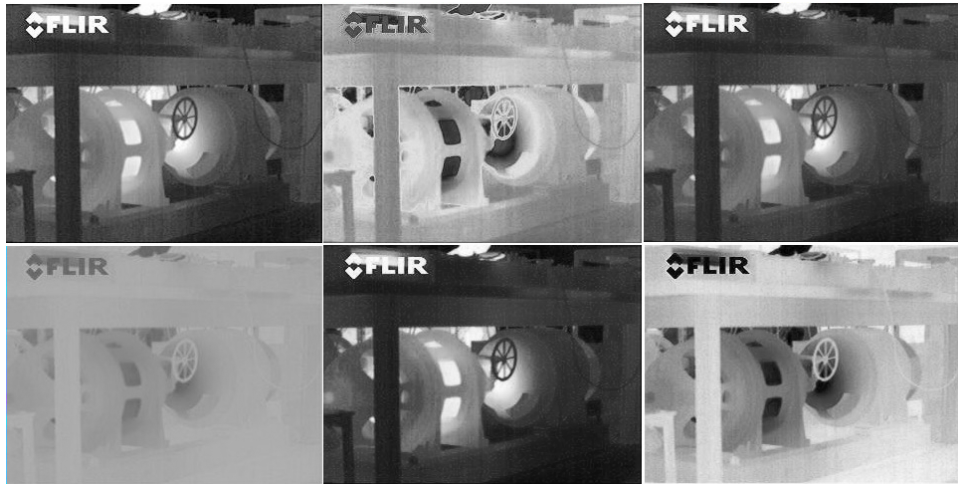
## 4.2 Thermographic inspections

INVIfusion 1.0 was conceived as a software tool to perform thermography inspections. This kind of inspections normally must accomplish with a standard, which defines the way to perform the inspection, the procedures to capture data, to show data and the kind of environmental data to register. The INVIfusion 1.0 software tool satisfies the thermography standards of the ASTM International (2014) for electrical and mechanical equipment. Then, the aim of this section is to show how Thermographic inspection data is organized in this report, which is generated by the report generation module shown in Figure 2c.

A Thermographic inspection was performed in the Electrical Machines Laboratory at the Universidad del Valle following the recommendations described in E07.10 (ASTM International, 2014). In this inspection, color and gray scale images (Figure 4a) were computed using the INVIfusion 1.0, as well as, different pseudo-color palettes (Rainbow, Iron, Cool, Hot, Iron with color inversion) for infrared images (Figure 4b). The hybrid camera setup was previously calibrated, this allows to the INVIfusion 1.0 performing the multimodal image fusion of the electrical devices present in the scene (Figure 4c). Then, using the GUI shown in Figure 2c users can generate the Thermographic inspection report. An example of this report is shown in Figure 5. Thanks to the images workspace shown in Figure 2b, the inspection report can include all taken and processed images such as infrared/visual spectrum histograms (Figure 4d), color threshold filtering (Figure 4d), visual spectrum edge extraction and their fusing with infrared images (Figure 4e), or multimodal image fusion of any inspected scene (Figure 4f).



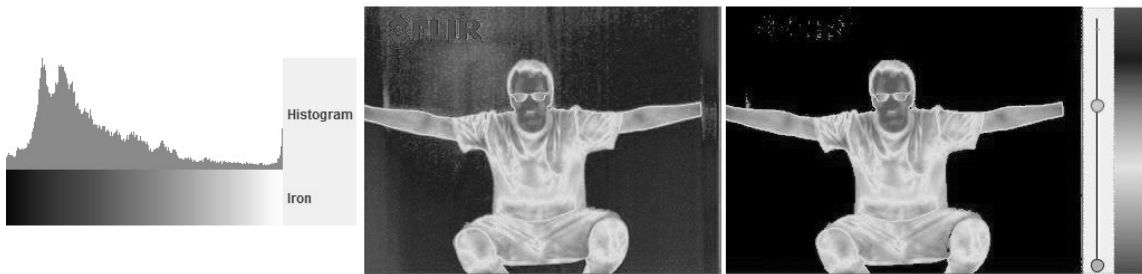
a.



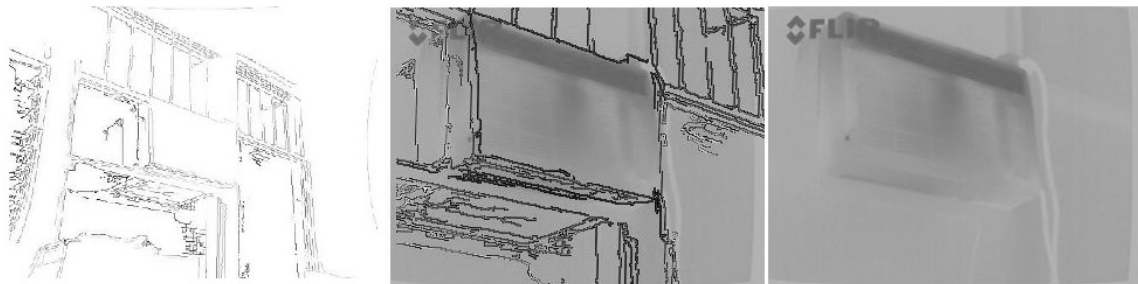
b.



c.



d.



e.



f.

**Figure 4.** a) Color and gray scale visualization. b) Different color palettes for infrared images. c) Visual and infrared multimodal images fusion for electrical equipment. d) Histogram and color thresholding. e) Edge extraction and multimodal image fusion. f) Outdoors visual and infrared multimodal images fusion.

### Reporte de Inspección Térmica de Laboratorio de Máquinas Eléctricas

<b>Empresa</b>	S Termografía Cll 22 # 2 - 23 Buena Vista	<b>Cliente</b>	Compañía ABC Cra 4 # 12 - 75 La Jungla
<b>Examinador</b>	Guillermo Herschel		

---

<b>Instrumento</b>	FLIR E320	No. Serie: 24301907	Objetivo: 27.4 mm
<b>Pedido</b>	Realizar una inspección térmica cualitativa en la ubicación del Laboratorio Eléctrico		

---

<b>Datos de imagen:</b>	Fecha: 15/11/2014	Grado de emisividad: 0.85	
	Hora: 10:43:14 a.m.	Temp. refl. [°C]: -	
	Archivo: vs_02.12-21.28.44.jpg		

---

Se debe continuar con el monitoreo de la tendencia de temperatura para buscar si existe cualquier anomalía.

---

**Conclusión:** En general, la instalación inspeccionada que se incorpora a este reporte se comenta en Condiciones Normales.

---

02/12/2014, \_\_\_\_\_  
**Guillermo Herschel**

**Figure 5.** Thermography report generated using the INVIFusion software according with the standard of the ASTM International (2014).

## 5. Conclusions

This work presents the INVIFusion 1.0 software tool for thermography inspection which fuses thermal and visual spectrum images using any hybrid camera setup (infrared and visual spectrum). INVIFusion is able to perform image processing tasks such as automatic intrinsic camera calibration; extrinsic camera calibration using a 2D Homography computation; diverse image processing tools to enhance thermal and visual images; thermal and visual image fusing; a report module to consolidate the thermography inspection results, and a friendly GUI to automate all these processes. The core of the INVIFusion software is the 2D homography computation, which is used to fuse infrared and visual spectrum image data. This method enables projecting pixel thermal data into visual spectrum images. As depicted in Table 1, this method was not explored in the discussed state of the art; this table also presents the current commercial solutions to handle hybrid camera setups. Unfortunately, none of these commercial solutions has a GUI to automate the extrinsic calibration process.

To validate the approach proposed in this work the MSRE was measured using all the corresponding points obtained from the calibration pattern. Hence, the proposed system shows a MSRE of  $2.08 \pm 1.8$  pixels in the worst case scenario. Also, different hybrid camera setups were tested obtaining similar results, which shows that the INVIFusion 1.0 software tool can deal with different infrared and visual spectrum camera configurations.

## 6. References

- Alahi, A., Ortiz, R. & Vandergheynst, P. (2012). *FREAK: Fast Retina Keypoint*. IEEE Conference on Computer Vision and Pattern Recognition, Rhode Island, USA, p. 510-517.
- ASTM International (2011). *C16.30, S. Standard Practice for Thermographic Inspection of Insulation Installations in Envelope Cavities of Frame Buildings*. <http://www.astm.org/Standards/C1060.htm>
- ASTM International (2014). *E07.10, S. Standard Guide for Examining Electrical and Mechanical Equipment with Infrared Thermography*. <http://www.astm.org/Standards/E1934.htm>
- Bay, H., Ess, A., Tuytelaars, T. & Van Gool, L. (2008). Speeded-up robust features (SURF). *Computer vision and image Understanding*. 110 (3), 346-359.
- Benitez, H., Loaiza, H., Caicedo, E., Bacca, B., Jimenez, H., Barreto, M. & Vargas, J. (2005). *Software Tool in Java for IR Image Processing: TermUV*. In: Proc. Vth International Workshop, Advances in Signal Processing for Non Destructive Evaluation of Materials, Quebec, Canada, p. 209-214.
- Bouguet, J.-Y. (2013). *Camera Calibration Toolbox for Matlab*. California Institute of Technology. [http://www.vision.caltech.edu/bouguetj/calib\\_doc/](http://www.vision.caltech.edu/bouguetj/calib_doc/)
- Fluke (2015a). *FLIR Tools Software for PC and Mac*. <http://www.flir.com/instruments/display/?id=54865>
- Fluke (2015b). *SmartView® Infrared Imaging Analysis and Reporting Software and Mobile App*. <http://www.fluke.com/fluke/r0en/accessories/Software/Fluke-SmartView-IR.htm?PID=56169>
- Harris, C. & Stephens, M. (1988). *A Combined Corner and Edge Detector*. In: Proceedings of the 4th Alvey Vision Conference. Manchester, U.K., p.174-151.
- Infrared, G. (2015). *Guide IR Analyzer*. [http://www.guideinfrared.com/Plus/m\\_default/Cms/default.php](http://www.guideinfrared.com/Plus/m_default/Cms/default.php)
- Kim, M., Han, D.K. & Ko, H. (2016). Joint patch clustering-based dictionary learning for multimodal image fusion. *Information Fusion*. 27, 198-214.
- Kruchten, P. (2003). *The Rational Unified Process: An Introduction*. 3rd ed. Indianapolis: Addison-Wesley Professional.
- Lowe, D.G. (2004). Distinctive Image Features from Scale-Invariant Keypoints. *International Journal of Computer Vision* 60 (2), 91-110.

- Ma, J., Chen, C., Li, C. & Huang, J. (2016). Infrared and visible image fusion via gradient transfer and total variation minimization. *Information Fusion* 31, 100-109.
- OpenCV (2014a). *Open Source Computer Vision*. <http://opencv.org/>
- Ospina Caicedo, R., Cardona Melo, S. & Bacca-Cortes, B. (2015). *INVIFusion*, Registro 13-48-353.
- Prakash, S., Lee, P.Y. & Caelli, T. (2006). *3D Mapping of Surface Temperature Using Thermal Stereo*. 9th International Conference on Control, Automation, Robotics and Vision, Singapore, p.1-4.
- Senya, P., Yoshinari, K. & Yuichi, O. (2011). *Infrared and Visible Spectrum Camera Calibration*. In: Proceedings of the IEICE General Conference 2011. Tsukuba: The Institute of Electronics, Information and Communication Engineers, Tokyo, Japan, p.104-112.
- St-Laurent, L., Prévost, D. & Maldague, X. (2010). *Fast and accurate calibration-based thermal/colour sensors registration*. Proceedings of 10th Quantitative InfraRed Thermography, Quebec, Canada, p.1-8.
- Strandemar, K. 762 94 R. (SE), (2013). *Resolution and contrast enhancement with fusion in IR images*. EP20120189618. <http://www.google.ch/patents/US9171361>
- Testo (2015). *Testo IrSoft*. <http://www.testo.com/>
- Trotec, (2015). *IC Report DuoVision*. [https://it.trotec.com/fileadmin/downloads/Temperaturtro\\_tr\\_ba\\_irreport\\_01\\_10\\_GB.pdf](https://it.trotec.com/fileadmin/downloads/Temperaturtro_tr_ba_irreport_01_10_GB.pdf)
- Ursine, W., Calado, F., Teixeira, G. & Diniz, H. (2012). *Thermal/Visible Autonomous Stereo Vision System Calibration Methodology for Non-controlled Environments*. Proceedings of 11th Quantitative InfraRed Thermography, Naples, Italy, p.1-10.
- Vidas, S. & Moghadam, P. (2013). HeatWave: A handheld 3D thermography system for energy auditing. *Energy and Buildings* 66, 445-460.
- Vidas, S., Moghadam, P. & Bosse, M. (2013). *3D thermal mapping of building interiors using an RGB-D and thermal camera*. 2013 IEEE International Conference on Robotics and Automation, Karlsruhe, Germany, p. 2311-2318.
- Yang, R. & Chen, Y. (2011). Design of a 3-D Infrared Imaging System Using Structured Light. *IEEE Transactions on Instrumentation and Measurement* 60 (2), 608-617.
- Yesner, R. (2013). *Smart Cities and the Internet of Everything: The Foundation for Delivering Next-Generation Citizen Services*. [http://www.cisco.com/c/dam/en\\_us/solutions/industries/docs/scc/ioe\\_citizen\\_svcs\\_white\\_paper\\_idc\\_2013.pdf](http://www.cisco.com/c/dam/en_us/solutions/industries/docs/scc/ioe_citizen_svcs_white_paper_idc_2013.pdf)
- Zhang, Z. (2000). A Flexible New Technique for Camera Calibration. *Pattern Analysis and Machine Intelligence, IEEE Transactions on* 22 (11), 1330-1334.
- Zhang, Z. & Way, O.M. (1999). *Flexible Camera Calibration By Viewing a Plane From Unknown Orientations*. In: Computer Vision, The Proceedings of the Seventh IEEE International Conference on. Kerkyra, Greece, p. 666-673.
- Zhao, J., Gao, X., Chen, Y., Feng, H. & Wang, D. (2016). Multi-window visual saliency extraction for fusion of visible and infrared images. *Infrared Physics & Technology* 76, 295-302.
- Zisserman, A. & Hartley, R. (2004). *Multiple view geometry in computer vision*. 2nd Edition. Cambridge: Cambridge University Press.



Revista Ingeniería y Competitividad por Universidad del Valle se encuentra bajo una licencia Creative Commons Reconocimiento - Debe reconocer adecuadamente la autoría, proporcionar un enlace a la licencia e indicar si se han realizado cambios. Puede hacerlo de cualquier manera razonable, pero no de una manera que sugiera que tiene el apoyo del licenciador o lo recibe por el uso que hace.